

Aalborg Universitet



AALBORG
UNIVERSITY

On Compliance and Buckling Objective Functions in Topology Optimization of Snap-Through Problems

Lindgaard, Esben; Dahl, Jonas

Published in:
Structural and Multidisciplinary Optimization

DOI (link to publication from Publisher):
[10.1007/s00158-012-0832-2](https://doi.org/10.1007/s00158-012-0832-2)

Publication date:
2013

Document Version
Accepted author manuscript, peer reviewed version

[Link to publication from Aalborg University](#)

Citation for published version (APA):
Lindgaard, E., & Dahl, J. (2013). On Compliance and Buckling Objective Functions in Topology Optimization of Snap-Through Problems. *Structural and Multidisciplinary Optimization*, 47(3), 409-421.
<https://doi.org/10.1007/s00158-012-0832-2>

General rights

Copyright and moral rights for the publications made accessible in the public portal are retained by the authors and/or other copyright owners and it is a condition of accessing publications that users recognise and abide by the legal requirements associated with these rights.

- Users may download and print one copy of any publication from the public portal for the purpose of private study or research.
- You may not further distribute the material or use it for any profit-making activity or commercial gain
- You may freely distribute the URL identifying the publication in the public portal -

Take down policy

If you believe that this document breaches copyright please contact us at vbn@aub.aau.dk providing details, and we will remove access to the work immediately and investigate your claim.

On compliance and buckling objective functions in topology optimization of snap-through problems

Esben Lindgaard · Jonas Dahl

Abstract This paper deals with topology optimization of static geometrically nonlinear structures experiencing snap-through behaviour. Different compliance and buckling criterion functions are studied and applied for topology optimization of a point loaded curved beam problem with the aim of maximizing the snap-through buckling load. The response of the optimized structures obtained using the considered objective functions are evaluated and compared. Due to the intrinsic nonlinear nature of the problem, the load level at which the objective function is evaluated has a tremendous effect on the resulting optimized design.

A well-known issue in buckling topology optimization is artificial buckling modes in low density regions. The typical remedy applied for linear buckling does not have a natural extension to nonlinear problems, and we propose an alternative approach. Some possible negative implications of using symmetry to reduce the model size are highlighted and it is demonstrated how an initial symmetric buckling response may change to an asymmetric buckling response during the optimization process. This problem may partly be avoided by not exploiting symmetry, however special requirements are needed of the analysis method and optimization formulation. We apply a nonlinear path tracing algorithm capable of detecting different types of stability points and an optimization formulation that handles possible mode switching. This is an extension into the topology optimization realm of a method developed, and used for, fiber angle optimization in laminated composite structures. We finally discuss and pinpoint some of the issues related to buckling topology optimization that remains unsolved and demands further research.

Keywords Topology optimization · Buckling · Structural stability · Critical load · Geometrically nonlinear · Design sensitivity analysis

1 Introduction

Since the introduction of the topology optimization method in the seminal paper Bendsøe and Kikuchi (1988), this method has been used to optimize a wide range of mechanical and non-mechanical problems. The reader is referred to the monograph Bendsøe and Sigmund (2003) for an excellent overview of this field. An important failure mode in structural elements is stability (buckling). Stability is especially critical for topology optimal designs that often are characterized by having a thin frame-like structure that inherently is prone to buckling. Only few topology optimization papers deal with stability and most of these are restricted to linear elastic structural responses. Furthermore, stability is often considered as a constraint in a stiffest design problem or an objective in a reinforcement problem. The focus of the present paper is maximization of structural buckling load using different compliance and buckling objective functions and comparison of the responses of the obtained designs. As geometrically nonlinear (GNL) modeling is applied, the load level at which the design sensitivities are evaluated is significant. Therefore, the compliance and buckling objective functions are evaluated at different load levels and the results of optimization are compared. A curved beam problem that exhibits snap-through behavior is used as an example of a generic buckling problem. We discuss some of the problems pertaining to optimization of buckling problems such as artificial local buckling modes and slow optimization convergence when using buckling load as the objective function instead of using buckling load as a constraint. Furthermore, some possible negative implications of exploiting symmetry

Esben Lindgaard (✉) · Jonas Dahl
Department of Mechanical and Manufacturing Engineering,
Aalborg University, Fibigerstraede 16,
DK-9220 Aalborg East, Denmark
E-mail: elo@m-tech.aau.dk

in the modeling of buckling problems for topology optimization, such as undetected mode switching, are demonstrated.

To the authors's knowledge the first work on optimization of buckling problems was Khot et al (1976) and Olhoff and Rasmussen (1977) where a linear modeling approach was employed for sizing of space truss structures and shape optimization of columns, respectively. This work was further developed and extended to topology problems in Neves et al (1995), Min and Kikuchi (1997), and Manickarajaha et al (2000). The topology optimization approach was extended into the geometrically nonlinear realm in Buhl et al (2000) where structures undergoing large displacements were optimized for stiffness. This work continued with optimization of nonlinear snap-through structures in Bruns et al (2002) and Bruns and Sigmund (2004). Geometrically nonlinear modeling was introduced in optimization of *buckling* problems in Sekimoto and Noguchi (2001) and Kemmler et al (2005). In the former article, structures are optimized to follow a certain load-displacement path, whereas in the latter article the compliance of the structures is minimized with a constraint on the lowest buckling load using an extended system of equations where the critical points are calculated directly.

In this paper we employ an alternative method originally introduced in Lindgaard and Lund (2010) and Lindgaard et al (2010) for nonlinear limit load buckling optimization of laminate composite shell structures using fiber angles as continuous design variables, and lately extended to handle both bifurcation and limit point instability in Lindgaard and Lund (2011). Optimization w.r.t. stability is accomplished by including the nonlinear response in the optimization formulation using a path tracing analysis. The nonlinear path tracing analysis is stopped when a stability point is encountered and the critical buckling load is approximated at a pre-critical load step according to the "one-point" approach, i.e. the stiffness information is extrapolated from *one* pre-critical equilibrium point until a singular tangent stiffness is obtained. Design sensitivities of the critical buckling load factors are obtained semi-analytically by the direct differentiation approach on the approximate eigenvalue problem described by discretized finite element matrix equations. A number of the lowest buckling load factors are considered in the optimization formulation in order to avoid problems related to "mode switching", i.e. the order of the eigenvalues in the buckling problem may change.

Simple stiffness criteria have also been studied in the attempt to improve the buckling load. Lee and Hinton (2000) studied linear strain energy minimization of shells with sizing and shape variables considering the improvement in nonlinear buckling limit load. They found for some examples an improvement in the nonlinear buckling load and for others a decrease and argued for the importance of accurately checking the stability limit of optimized shell structures by ge-

ometrically nonlinear analysis. To further examine this we benchmark different linear and nonlinear stiffness criteria against the nonlinear buckling formulation with the aim of improving the buckling resistance.

A known problem in topology optimization of buckling problems is that local artificial buckling modes may emerge in low-density regions during the optimization process, see Neves et al (1995, 2002). The standard solution for linear problems is to use different penalization schemes for the linear stiffness and the stress stiffness matrices. In section 3, we show that this approach does not have a natural extension to nonlinear buckling problems due to inconsistencies within the equilibrium problem and within the design sensitivity analysis and we discuss alternative approaches.

The structure of the present paper is as follows: In section 2 we describe the used computational approach for static and buckling analysis for the geometrically linear and nonlinear case. In section 3, we give a brief overview of the topology optimization method as it is used in this paper. In sections 4 and 5 we introduce the different compliance and buckling based objective functions and associated optimization formulations that are compared in the numerical studies in section 6. The paper concludes with a discussion of the main findings in the numerical studies.

2 Static and buckling analysis

The finite element method is used for determining the buckling load of the structure, thus the derivations are given in a finite element context. The applied finite element is a standard displacement based eight node isoparametric plane stress solid element.

2.1 Linear static and buckling analysis

Linear buckling analysis is a classical engineering method for determining the buckling load of structures. The method gives numerical inexpensive predictions of buckling with stability point, i.e. singular tangent stiffness. Linear buckling analysis is based upon linear static analysis where the static equilibrium equation for the structure may be written as

$$\mathbf{K}_0 \mathbf{D} = \mathbf{R} \quad (1)$$

Here \mathbf{D} is the global displacement vector, \mathbf{K}_0 is the global initial stiffness matrix, and \mathbf{R} the global load vector.

Based on the displacement field, obtained by the solution to (1), the element stresses can be computed, whereby the stress stiffening effects due to mechanical loading can be evaluated by computing the initial stress stiffness matrix \mathbf{K}_σ . By assuming the structure to be perfect with no geometric imperfections, stresses are proportional to the loads, i.e.

stress stiffness depends linearly on the load, displacements at the critical/buckling configuration are small, and the load is independent of the displacements, the linear buckling problem can be established as

$$(\mathbf{K}_0 + \lambda_j \mathbf{K}_\sigma) \phi_j = \mathbf{0}, \quad j = 1, 2, \dots, J \quad (2)$$

where the eigenvalues are ordered by magnitude, such that λ_1 is the lowest eigenvalue, i.e. buckling load factor, and ϕ_1 is the corresponding eigenvector, i.e. buckling mode. In general the eigenvalue problem in (2) can be difficult to solve, due to the size of the matrices involved and large gaps between the distinct eigenvalues. For efficient and robust solutions, equation (2) is solved by a subspace method with automatic shifting strategy, Gram-Schmidt orthogonalization, and the sub-problem is solved by the Jacobi iterations method, see Wilson and Itoh (1983).

2.2 Geometrically nonlinear static and buckling analysis

Better predictions of structural buckling with stability points than that available by linear buckling analysis may be achieved by nonlinear buckling analysis. The method incorporates geometrically nonlinear analyses and applies for both bifurcation and limit point instability. The proposed procedure for nonlinear buckling analysis is schematically shown in Fig. 1 and consists of the steps stated in Algorithm 1. During a geometrically nonlinear analysis the fundamental stability point is detected if it exists. Two stability situations are depicted in Fig. 1: an unstable bifurcation point and a load limit point. In both cases the stability point is detected by the procedures described in Sect. 2.2.1.

Algorithm 1 Pseudo code for the nonlinear buckling analysis

- 1: Geometrically nonlinear (GNL) analysis by arc-length method
- 2: Monitor and detect stability point during GNL analysis
- 3: Re-set all state variables to configuration at load step just before stability point - a precritical point
- 4: Perform eigenbuckling analysis on deformed configuration at load step before stability point

We consider geometrically nonlinear behaviour of structures made of linear elastic materials. We adopt the Total Lagrangian approach, i.e. displacements refer to the initial configuration, for the description of geometric nonlinearity and use the nonlinear Green-Lagrange strain measure together with the work consistent second Piola-Kirchhoff stress. An incremental formulation is suitable for nonlinear problems and it is assumed that the equilibrium at load step n is known and that the equilibrium at load step $n + 1$ is desired. Furthermore, it is assumed that the current load is independent on deformation. The incremental equilibrium equation in the

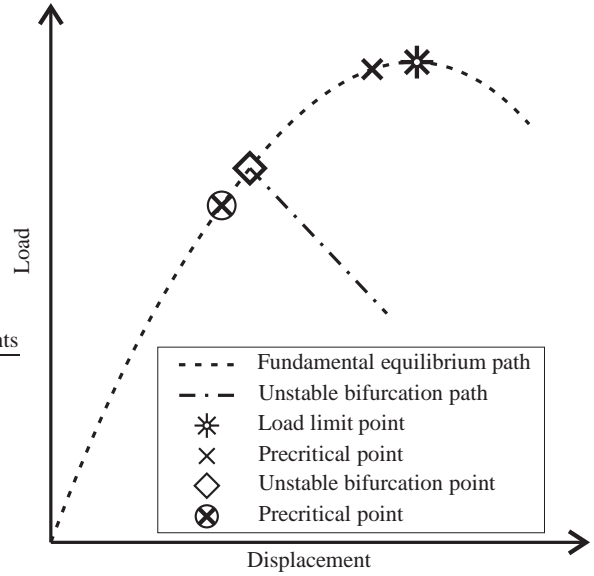


Fig. 1 Detection of stability point in step 2 and chosen precritical equilibrium point for the nonlinear buckling problem in case of unstable bifurcation and limit point instability.

Total Lagrangian formulation is written as (see e.g. Brendel and Ramm (1980); Hinton (1992))

$$\mathbf{K}_T(\mathbf{D}^n, \gamma^n) \delta \mathbf{D} = \mathbf{R}^{n+1} - \mathbf{F}^n \quad (3)$$

$$\mathbf{K}_T(\mathbf{D}^n, \gamma^n) = \mathbf{K}_0 + \mathbf{K}_L(\mathbf{D}^n, \gamma^n) + \mathbf{K}_\sigma(\mathbf{D}^n, \gamma^n) \quad (4)$$

$$\mathbf{K}_T^n = \mathbf{K}_0 + \mathbf{K}_L^n + \mathbf{K}_\sigma^n \quad (5)$$

Here $\delta \mathbf{D}$ is the incremental global displacement vector, \mathbf{F}^n global internal force vector, and \mathbf{R}^{n+1} global applied load vector. The global tangent stiffness \mathbf{K}_T^n consists of the global initial stiffness \mathbf{K}_0 , the global stress stiffness \mathbf{K}_σ^n , and the global displacement stiffness \mathbf{K}_L^n . The applied load vector \mathbf{R}^n is controlled by the stage control parameter (load factor) γ^n according to an applied reference load vector \mathbf{R}

$$\mathbf{R}^n = \gamma^n \mathbf{R} \quad (6)$$

The incremental equilibrium equation (3) is solved by the arc-length method, Crisfield (1981). During the nonlinear path tracing analysis we can at some converged load step estimate an upcoming critical point, i.e. bifurcation or limit point, by utilizing tangent information. At a critical point the tangent operator is singular

$$\mathbf{K}_T(\mathbf{D}^c, \gamma^c) \phi_j = \mathbf{0} \quad (7)$$

where the superscript c denotes the critical point and ϕ_j the buckling mode. To avoid a direct singularity check of the tangent stiffness, it is convenient to utilize tangent information at some converged load step n and extrapolate it to the critical point. The one-point approach only utilizes information at the current step and extrapolates by only one point, see Brendel and Ramm (1980) and Borri and Hufendiek (1985). The stress stiffness part of the tangent stiffness at the

critical point is approximated by extrapolating the nonlinear stress stiffness from the current deformed configuration as a linear function of the load factor γ .

$$\mathbf{K}_\sigma(\mathbf{D}^c, \gamma^c) \approx \lambda \mathbf{K}_\sigma(\mathbf{D}^n, \gamma^n) = \lambda \mathbf{K}_\sigma^n \quad (8)$$

It is assumed that the part of the tangent stiffness consisting of \mathbf{K}_L^n and \mathbf{K}_0 does not change with additional loading, which holds if the additional displacements relative to the current deformed configuration are small. The tangent stiffness at the critical point is approximated as

$$\mathbf{K}_T(\mathbf{D}^c, \gamma^c) \approx \mathbf{K}_0 + \mathbf{K}_L^n + \lambda \mathbf{K}_\sigma^n \quad (9)$$

and by inserting into (7) we obtain a generalized eigenvalue problem

$$(\mathbf{K}_0 + \mathbf{K}_L^n) \phi_j = -\lambda_j \mathbf{K}_\sigma^n \phi_j \quad (10)$$

where the eigenvalues are assumed ordered by magnitude such that λ_1 is the lowest eigenvalue and ϕ_1 the corresponding eigenvector. The solution to (10) yields the estimate for the critical load factor at load step n as

$$\gamma_j^c = \lambda_j \gamma^n \quad (11)$$

If $\lambda_1 < 1$ the first critical point has been passed by the path tracing analysis and if $\lambda_1 > 1$ the critical point is upcoming. The one-point procedure works well for both bifurcation and limit points. The closer the current load step gets to the critical point, the better the approximation becomes, and it converges to the exact result in the limit of the critical load.

2.2.1 Stop criteria in GNL analysis

Several different stop criteria are applied for the GNL analyses from which an equilibrium point is determined for the design sensitivity analysis during the optimization. In the case of buckling with a stability point in the form of a limit point, a limit point detector criterion may be used. The limit load is simply detected by monitoring the load factor in the GNL analysis, see (3). When the load factor from two successive load steps decreases the previous converged load is defined as the limit load. A bifurcation point detector, as described in Lindgaard and Lund (2011), may be applied in case of bifurcation buckling. For bifurcation point detection, nonlinear buckling analysis by (10) is performed at precritical stages during GNL analysis as a singularity check on the tangent stiffness. Finally the GNL analysis may be stopped at a prescribed load level. This stop criterion is applied to investigate the effect of evaluating the design sensitivities close or far away from the buckling point.

3 Topology optimization approach

The goal of a structural topology problem is to determine the optimal material distribution layout, i.e. the optimal material density distribution ρ within a given design domain that minimizes a given objective function subject to prescribed constraint functions. Here, the design domain is defined by a continuum discretized by finite elements, thus reducing the topology problem to determination of the densities within each finite element ρ_e . The density variable may take the values from zero to one, i.e. void to solid material. The material model of the finite element is related to the density variables through weight functions w_e also known as material interpolation schemes

$$\mathbf{E}_e^{\text{eff}} = w_e \mathbf{E} \quad (12)$$

$$V_e^{\text{eff}} = w_e V_e \quad (13)$$

where \mathbf{E} is a reference constitutive matrix of the bulk material and V_e is the element volume. A selection of different material interpolation schemes is stated in Table 1. The

Table 1 Material interpolation schemes, w_e . The density variable ρ_e may take the values $0 < \underline{\rho}_e \leq \rho_e \leq 1$, where $\underline{\rho}$ is a minimum density value, typically $\underline{\rho} = 0.001$, to avoid a singular structural stiffness matrix.

Scheme #	Weight function, w_e
1	$w_e = \rho_e$
2	$w_e = \rho_e^p$
3	$w_e = \rho_{min} + (1 - \rho_{min})\rho_e^p$
4	$w_e = 0$ if $\rho_e < \rho_{cutoff}$ $w_e = \rho_e^p$ if $\rho_e \geq \rho_{cutoff}$

most simple material model would be a linear scaling (scheme 1) of the stiffness and volume according to the density variable ρ_e . This approach leads to optimal designs containing many grey areas which are unwanted. In order to obtain integer 0-1 solutions that may be manufactured with bulk material, i.e. solutions containing only void and solid, penalization of the objective function for intermediate densities can be introduced. The very popular SIMP-approach (Solid Isotropic Material with Penalization) (scheme 2), see Bendsoe (1989); Rozvany et al (1992); Bendsoe and Sigmund (1999, 2003), is applied only to the stiffness interpolation in (12) and penalizes the objective function implicitly when the penalization parameter $p > 1$. In this work we apply SIMP (scheme 2) for all stiffest structural design problems.

Artificial modes may appear in low density regions when the stress stiffness, \mathbf{K}_σ , becomes high compared to the ini-

tial stiffness, \mathbf{K}_0 , thus producing localized artificial buckling modes. For linear buckling topology optimization one of two approaches is normally applied in order to circumvent problems with artificial buckling modes in low density regions. Both approaches apply different material interpolation schemes on different stiffness terms in the static problem and in the buckling problem. The approach proposed by Neves et al (1995) is simply to ignore the stress stiffness contribution of low density elements by applying scheme 2 for initial stiffness \mathbf{K}_0 and scheme 4 for stress stiffness \mathbf{K}_σ , where ρ_{cutoff} defines a cutoff value on the element densities. Since this approach may give rather abrupt changes in the values of the objective and design sensitivities and thereby cause oscillations of the optimization, Bendsøe and Sigmund (2003) proposed a differentiable version of the approach by introducing a slightly different smooth interpolation of the initial stiffness term as,

$$\begin{aligned} \text{For } \mathbf{K}_0 : \quad \mathbf{E}_0^{\text{eff}} &= w_e^3 \mathbf{E} = [\rho_{\min} + (1 - \rho_{\min})\rho_e^p] \mathbf{E} \\ \text{For } \mathbf{K}_\sigma : \quad \mathbf{E}_\sigma^{\text{eff}} &= w_e^2 \mathbf{E} = [\rho_e^p] \mathbf{E} \end{aligned} \quad (14)$$

where scheme 2 is applied for stress stiffness and scheme 3 is applied for initial stiffness. The ρ_{\min} is set such that problems with artificial modes are avoided when the element densities ρ_e are around their lower bound value $\underline{\rho}$. However, a too large ρ_{\min} results in unrealistic high stiffness of the supposedly void elements. In this work we apply the interpolation schemes in (14) in order to avoid artificial buckling modes in the linear buckling problem.

In the case of nonlinear buckling, see (10), it is tempting to use a similar approach by stating that

$$\begin{aligned} \text{For } \mathbf{K}_0 : \quad \mathbf{E}_0^{\text{eff}} &= w_e^3 \mathbf{E} = [\rho_{\min} + (1 - \rho_{\min})\rho_e^p] \mathbf{E} \\ \text{For } \mathbf{K}_L : \quad \mathbf{E}_L^{\text{eff}} &= w_e^3 \mathbf{E} = [\rho_{\min} + (1 - \rho_{\min})\rho_e^p] \mathbf{E} \\ \text{For } \mathbf{K}_\sigma : \quad \mathbf{E}_\sigma^{\text{eff}} &= w_e^2 \mathbf{E} = [\rho_e^p] \mathbf{E} \end{aligned} \quad (15)$$

This will however lead to inconsistencies between the residual, \mathbf{Q} , and the tangent stiffness, \mathbf{K}_T , which can result in slow convergence or even non-convergence of the static problem, since

$$\mathbf{K}_T^n \delta \mathbf{D} = \mathbf{R}^{n+1} - \mathbf{F}^n = -\mathbf{Q} \quad (16)$$

$$\frac{\partial \mathbf{Q}}{\partial \mathbf{D}} \equiv \mathbf{K}_T^n = \mathbf{K}_0 + \mathbf{K}_L^n + \mathbf{K}_\sigma^n \quad (17)$$

The inconsistencies arise due to the fact that the inner forces contained in the residual are based upon the element stresses which are not uniquely defined when using the aforementioned interpolation scheme. Similar inconsistencies arise in the design sensitivity analysis of the nonlinear buckling problem in (10) when using different material interpolation schemes for the different tangent stiffness terms.

The success of the approach in the case of the linear buckling problem is due to the fact that the linear static problem in (1) and the linear buckling problem in (2) are weakly coupled, i.e. the nonlinear stress stiffness is assumed to behave linearly with respect to the applied loading and not influence the deformation configuration of the static problem. For the nonlinear buckling problem there is a strong coupling between the tangent stiffness terms and the deformation configuration, and thus a strong coupling between the static problem in (3) and the buckling problem in (10), which makes the above approach unsuitable.

To avoid artificial buckling modes and to ensure consistency in the geometrically nonlinear static problem, in the case of nonlinear buckling topology optimization, we propose to apply material interpolation scheme 3 to *all* tangent stiffness terms as well as to the residual. This seems to eliminate problems with artificial buckling modes such that (10) produces *real* structural buckling modes, while retaining consistency in the static problem and design sensitivity analysis. Furthermore, we have not observed any convergence difficulties in the geometrically nonlinear static problem due to low density regions. It does, however, result in a slightly overly stiff structure due to the remaining stiffness of low density elements. Since ρ_{\min} in scheme 3 is set very low, typically the same as the lower bound density $\underline{\rho}$, this does not seem to influence the results significantly.

Filtering and continuation approach

The well-known problems with checker boarding due to the use of low order elements which are prone to shear locking have been avoided by the use of quadratic elements and thus no filtering techniques have been applied in this work. This means that the obtained designs are mesh-dependent. This is, however, not considered a problem since the finite element mesh is kept fixed in all numerical studies and the scope of the present work is to compare different performance criteria used in topology optimization.

It is well-known that the resulting topologies to some extent depend on choices of optimization parameters and starting guessing. In order to counteract this problem we apply a continuation approach, see Buhl et al (2000); Bendsøe and Sigmund (2003), for the control of the penalty parameter p in Table 1. The penalty parameter is initially set to $p = 1$ and gradually increased to a value of $p = 3$ during the optimization process. For $p = 1$ it resembles the so-called variable-thickness-sheet problem having many grey areas, i.e. elements with intermediate densities, which at least for the linear compliance problem is known to be a convex problem.

4 Objective functions

A range of different objective functions are investigated and considered for maximization of the lowest buckling load. The objective functions are described in the following and comments about the design sensitivity analysis of the different objective functions are given. The equations for the design sensitivity analysis are stated in Appendix A.

4.1 Linear compliance

Linear compliance C_L is defined as the work done by the applied loads at the equilibrium state expressed in terms of the linear static equilibrium equation stated in (1).

$$C_L(\mathbf{D}) = \mathbf{R}^T \mathbf{D} \quad (18)$$

4.2 Nonlinear end compliance

Nonlinear end compliance C_{GNL} is defined as the work done by the applied loads at the equilibrium state at the final load step n expressed in terms of the nonlinear incremental equilibrium equation stated in (3).

$$C_{GNL}(\mathbf{D}^n, \mathbf{R}^n) = (\mathbf{R}^n)^T \mathbf{D}^n \quad (19)$$

The expression for the nonlinear end compliance in (19) is in general dependent on both the displacements, \mathbf{D}^n and the external load, \mathbf{R}^n at the final load step n . Considering design changes, the nonlinear end compliance criterion applied in this study is only considered dependent upon the displacements \mathbf{D}^n at the chosen load step n whereas the applied load \mathbf{R}^n is considered independent upon design changes, i.e. $C_{GNL}(\mathbf{D}^n(\boldsymbol{\rho}), \mathbf{R}^n)$ where the design variables $\rho_e, e = 1, \dots, N_e$, are collected in $\boldsymbol{\rho}$.

4.3 Linear buckling

The linear buckling load is obtained as the lowest eigenvalue of (2). Traditionally, the linear buckling load is considered as objective when the task is to improve the buckling resistance of structures and therefore applied in the study as a frame of reference. However, for topology optimization problems, linear buckling is typically applied as a constraint in a stiffness design problem or as objective in a reinforcement problem. Thus, studies with linear buckling as objective in general topology optimization problems are limited.

4.4 Nonlinear buckling

The nonlinear buckling load is determined at a precritical load level using the one-point approach by solving the eigenvalue problem in (10) and estimating the buckling load by linear extrapolation in (11). Better predictions of the buckling load are generally obtained by nonlinear buckling analysis compared to the traditional linear buckling analysis. Conversely, nonlinear buckling analysis is more complicated and numerical expensive than linear buckling analysis since it requires geometrically nonlinear analysis to trace the equilibrium path. The nonlinear buckling load is formulated as an objective function by the procedures originally proposed in Lindgaard and Lund (2010) and Lindgaard et al (2010). The expressions for the design sensitivities are as for the other objective functions described in Appendix A. In this work only simple eigenvalues have been considered since multiple eigenvalues have not been encountered in the numerical studies. In case of multiple eigenvalues the sensitivities may be computed and handled by the methodologies proposed by Seyranian et al (1994); Neves et al (1995); Du and Olhoff (2007).

5 Optimization problem formulations

Two types of optimization formulations are applied in this study in the attempt to improve the buckling resistance using topology optimization. The design variables in the numerical studies are the element topology density variables ρ_e . In case of compliance objective the problem is formulated as a simple minimization problem based on either linear or geometrically nonlinear analysis.

$$\text{Objective : } \min_{\boldsymbol{\rho}} C$$

$$\text{Subject to : State equation (1) or (3)}$$

$$\begin{aligned} \sum_{e=1}^{N_e} \rho_e V_e &\leq \bar{V} \\ 0 < \underline{\rho}_e &\leq \rho_e \leq 1, \quad e = 1, \dots, N_e \end{aligned}$$

where ρ_e and V_e , respectively, denote the density variable and volume of element e , \bar{V} is the maximum allowable volume, and $\underline{\rho}_e$ is lower bound density value ($\underline{\rho}_e = 0.001$) to avoid a singular structural stiffness matrix.

In case of buckling objective the optimization problem is formulated as a max-min problem. The direct formulation of the optimization problem in the case of the max-min problem can give problems related to differentiability and fluctuations during the optimization process due to “mode switching”, i.e. the order of the eigenvalues in the buckling problem may change, e.g. the second lowest eigenvalue can become the lowest. An elegant solution to this problem is to

make use of the so-called bound formulation, see Bendsøe et al (1983), Taylor and Bendsøe (1984), and Olhoff (1989). A new artificial variable β is introduced as a new objective function. An equivalent problem is formulated, where the previous non-differentiable objective function is transformed into a set of constraints. In the case of either linear or nonlinear buckling objective, the mathematical programming problem is formulated as

$$\text{Objective : } \max_{\rho, \beta} \beta$$

$$\text{Subject to : } \gamma_j^c \geq \beta, \quad j = 1, \dots, N_\lambda$$

$$\text{State equation (1), (2) or (3), (10)}$$

$$\sum_{e=1}^{N_e} \rho_e V_e \leq \bar{V}$$

$$\underline{\rho}_e \leq \rho_e \leq \bar{\rho}_e, \quad e = 1, \dots, N_e$$

The mathematical programming problems are solved by the Method of Moving Asymptotes (MMA) by Svanberg (1987). The closed loop of analysis, design sensitivity analysis and optimization is repeated until convergence of the design variables or until the maximum number of allowable iterations has been reached.

6 Generic 2D curved beam problem

A generic plane stress buckling problem of a curved beam, see Fig. 2, is applied in this study. 2040 standard 2D 8-noded

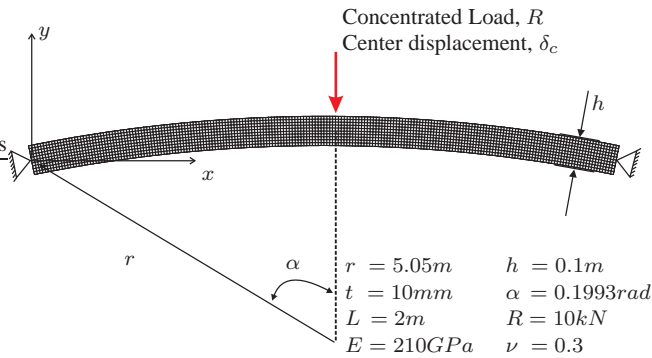


Fig. 2 Geometry, loads, boundary conditions, and material properties for the 2D curved beam problem.

quadratic isoparametric displacement based finite elements are used to model the entire beam. The volume constraint for the topology optimization is set to 50% of the initial design. The structural response of the initial grey topology design with all element densities set to $\rho_e = 0.5$ and a penalty parameter of $p = 1$ is shown in Fig. 3. The stability of the initial design is governed by a snap-through limit point instability with a symmetric buckling mode behaviour. Asymmetric buckling responses in the form of bifurcation-type

instabilities are not present for the initial design. Therefore, symmetry is applicable to reduce the model size for the initial design. In the optimization studies two configurations of the beam are considered; a symmetric model and a full model. In the symmetric model only a half beam is analysed by applying symmetry boundary conditions along the symmetry line (marked with a hatched line in Fig. 2). The full model is utilized to investigate whether asymmetric effects are introduced during optimization of the symmetric model.

6.1 Optimization of symmetric model

For the symmetric model a range of different optimization formulations based upon different objective functions with the aim of maximizing the lowest buckling load is benchmarked. These include linear compliance, nonlinear end compliance, and nonlinear buckling load. In order to study the influence of the chosen load level for the compliance minimization, three optimizations have been performed

- 1: Linear compliance
- 2: Nonlinear end compliance at limit point
- 3: Nonlinear end compliance at postbuckling load ($\gamma = 30$)

Optimum topologies and their final equilibrium curves from the topology optimization studies on the symmetric model are shown in Fig. 3. The optimum topologies for optimizations 1-3, which all have compliance type objective functions, are very different from each other and so are their structural performance. Optimization 2, which minimizes nonlinear end compliance at the limit load, has a higher buckling load than optimization 1 which minimizes linear compliance. Optimization 3 minimizes nonlinear end compliance in the postbuckling regime at a load factor of $\gamma = 30$. Here the displacement configuration of the structure is completely different since its shape is fully inverted and thereby nearly perfectly loaded in a tension membrane fashion. The obtained topology design by this optimization is completely different from those from optimization 1 and 2 and has a much lower snap-through buckling load but a much higher postbuckling stiffness. This clearly demonstrates the importance of geometrically nonlinear effects and that special care should be devoted to choosing a proper load level for the stiffness optimization. This is due to the fact that the load level dictates the displacement configuration and that the compliance minimization thereby maximises the stiffness according to that displacement configuration.

Finally, the limit point buckling load has been optimized directly by the nonlinear buckling load criterion in optimization 4. The topological design and structural performance is very similar to optimization 2, thus minimum end compliance at the limit load seems to be a good criterion for improvement of the buckling performance.

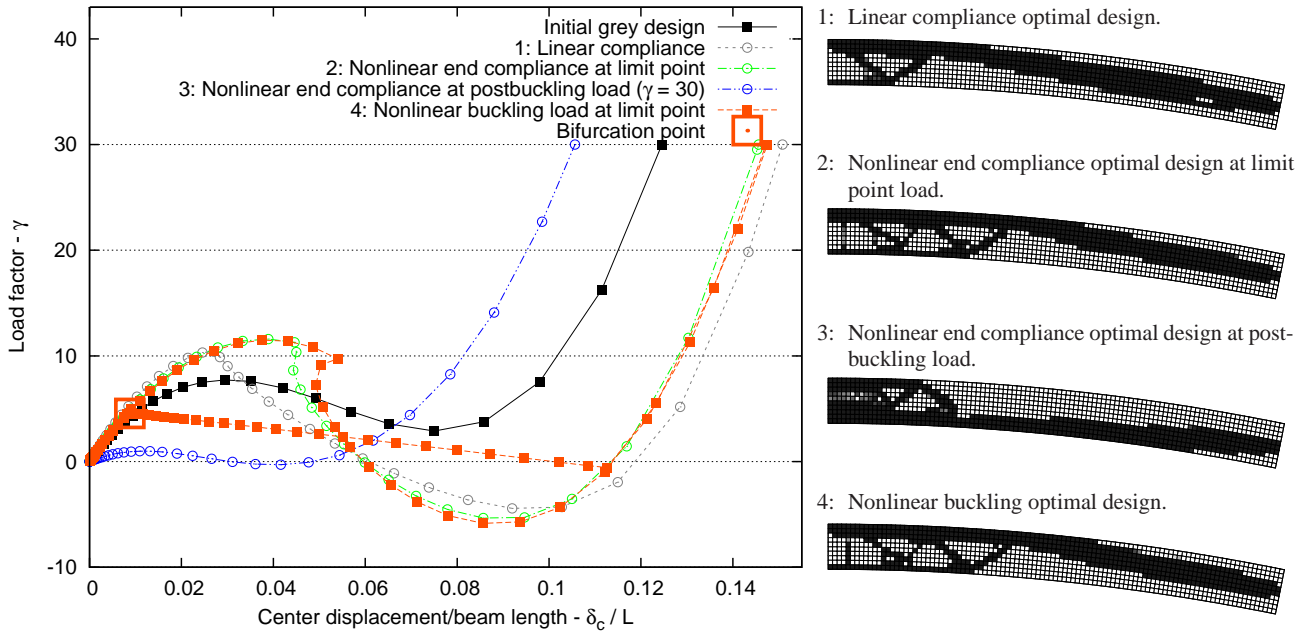


Fig. 3 Load-deflection curves for optimum designs of symmetric model obtained by geometrically nonlinear analysis.

To validate the designs, full models are generated by mirroring the topological designs and complete geometrically nonlinear assessments are carried out. Surprisingly, it turns out that new stability points of the bifurcation type have been introduced during the optimization for optimization 1-4. The consequence of this is that the bifurcation buckling load for optimization 4 is less than half of the limit point buckling load. The loading point, secondary path, and buckling mode for the bifurcation point are shown in Fig. 3 and 4, respectively. For the sake of clarity, the secondary path and buckling mode are only shown for optimization 4. The bifurcation buckling load factors for optimization [1; 2; 3; 4] are $\gamma_{bif}^c = [4.25; 4.45; 0.76; 4.55]$, and are all well below the limit point buckling load factors of the designs.



Fig. 4 Asymmetric bifurcation buckling mode of optimal design from optimization 4 on symmetric model.

This clearly demonstrates that special care should be taken when applying symmetry even though the initial design has a completely symmetric structural response. This is due to the fact that the validity of the symmetry conditions may be altered during the optimization process. This also means that the obtained designs by compliance minimization cannot be trusted when there is the risk that new stability points may be introduced during optimization. This is also the case when minimizing compliance of a full model,

since a path tracing algorithm in a geometrically nonlinear analysis typically just traces the fundamental equilibrium path, which corresponds to a symmetric response, without the capability to detect critical points. Therefore, dedicated methods which incorporate special features in the analysis method and optimization formulation are required in order to reliably deal with this problem. Such a method is described and applied in the following for topology optimization of a full model of the curved beam.

6.2 Optimization of full model

The full model is now considered for nonlinear buckling topology optimization and referred to as optimization 5. Here the nonlinear buckling load criterion is applied as objective and set up to handle both bifurcation and/or limit point buckling. The numerical procedure in optimization 5 is as follows: First, a nonlinear buckling analysis is performed by the procedure described in Algorithm 1 taking geometrically nonlinear prebuckling deformations into account. The nonlinear buckling problem in (10) is solved at the deformed configuration just before the critical point, i.e. limit point or bifurcation point, and the design sensitivities are evaluated for a specific number of buckling loads, thus taking care of possible mode switching during the optimization process via the use of the bound formulation. Finally, the MMA optimizer makes a design update and the procedure is repeated until convergence.

During optimization 5 it has been verified that the fundamental critical buckling mode changes during the optimization

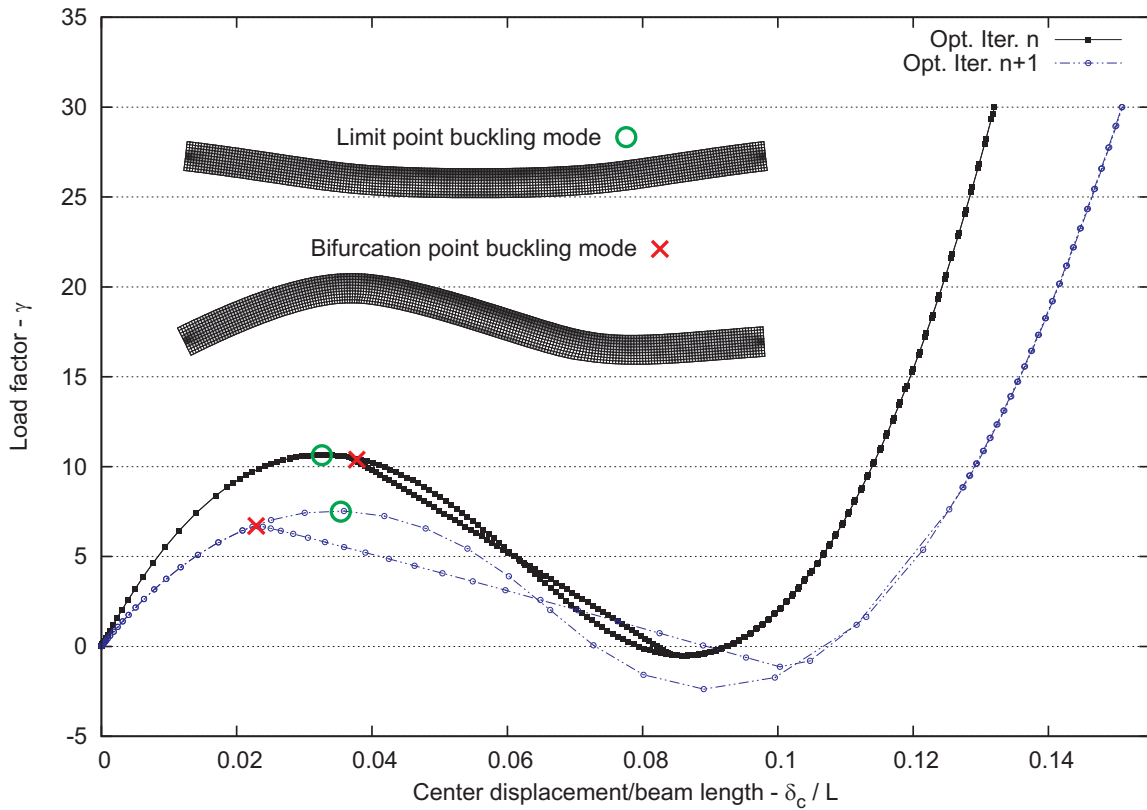


Fig. 5 Structural responses of two successive designs from the topology optimization of the full model of the curved beam using the nonlinear buckling optimization formulation (optimization 5). It is verified that mode switching takes place during the optimization process. Note that the drop in buckling load and structural stiffness is due to an increase in the penalty parameter p used in the material interpolation scheme.

tion process as suggested by the studies of the symmetric model. This is clearly illustrated in Fig. 5 where the structural responses from complete geometrically nonlinear assessments are depicted from two successive designs during the optimization process of optimization 5. At first, the fundamental buckling mode is governed by a limit point instability which has a symmetric response. After reaching this limit point a bifurcation point appears on the unstable path of the equilibrium curve. In the next design iteration the critical points have changed position such that the bifurcation point related to an asymmetric mode now has become the fundamental one. Note that the reason for the decrease in overall buckling load and stiffness of the structure between the two design iterations is due to an increase in the penalty parameter used in the material interpolation scheme. During the remainder of optimization 5 a number of incidents with mode switching have been observed. This however did not result in any oscillating behaviour of the objective function since mode switching effectively is dealt with by the use of the bound formulation. From this it is clear that the application of symmetry will give misleading optimization results and that an advanced method that is capable of dealing with both types of instabilities and possible mode switching is needed.

The final optimized topology design from optimization 5 is shown in Fig. 6 together with its equilibrium curve and structural response characteristics. This design is completely different from those from optimization 1-4 by that it is fully reinforced along the top and bottom edge of the beam which gives it high bending stiffness. The buckling load of this design is $\gamma^c = 10.49$ and over twice as high (actually 131% higher) as the best designs from optimization 1-4 which have bifurcation buckling load factors of $\gamma_{bif}^c \leq 4.55$.

From the deformation modes shown in Fig. 6, which match the depicted equilibrium configurations, it is observed that the beam initially deforms symmetrically. When the limit point is reached the structure starts to deform asymmetrically and continues to do so throughout the entire unstable part of the equilibrium curve. Finally, the structural shape is fully inverted (concave, rather than the convex undeformed shape) and the structural response again becomes symmetric on the postbuckling stable part of the equilibrium curve. Note that during global buckling of the beam a couple of local struts within the beam buckle locally. It may be observed that the design is not fully symmetric indicating that this is not the global optimal solution. The authors expect the global optimum design to be symmetric since the fundamental buckling response is a symmetric point of bifurca-

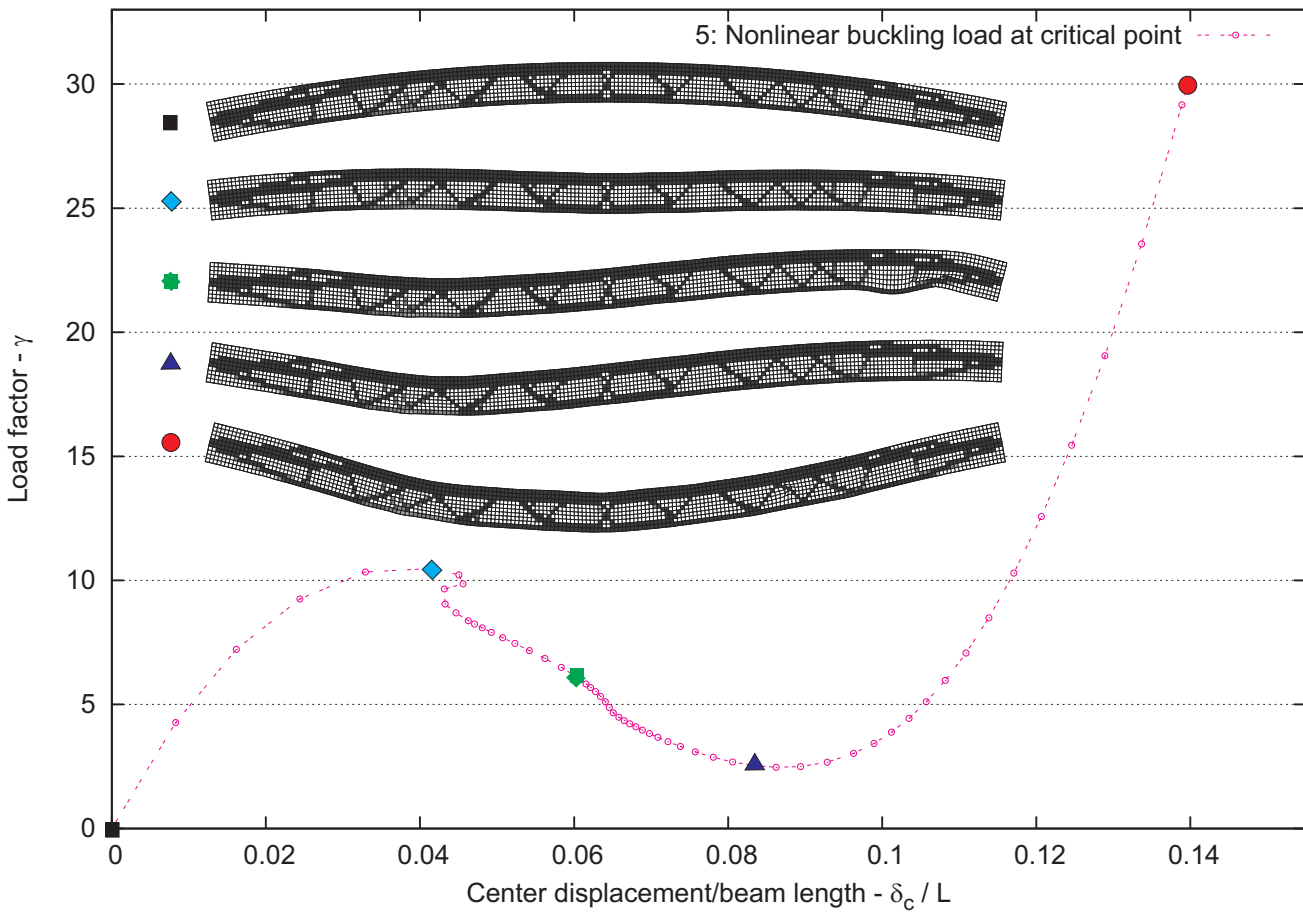


Fig. 6 Determined optimum topology from optimization 5 on the full beam model together with its equilibrium curve and structural response characteristics.

tion associated with asymmetric deformation response. This means that the structure ideally should have same resistance against positive and negative asymmetric deflections. Solution of this problem was very hard and required many iterations in order to get a nearly black and white design which partly can be explained by switching buckling modes during the optimization process and that the optimal solution seems to be a design where several parts of the structure buckles simultaneously.

Linear buckling optimization of the full model of the curved beam has also been performed though with quite poor results, since it resulted in degenerated optimized designs with many grey areas and a disconnected structure. In order to obtain physical structural designs, a compliance constraint can be added to the linear buckling problem, which ensures a connected structure, i.e. a load path between the applied loading and boundary conditions. However, the structural design then becomes a compromise between two criteria, and the needed compliance threshold is model dependent. From our findings, a strict compliance constraint is needed to drive the optimization problem towards a valid physical design when using this approach.

7 Conclusions

The focus of this work is to investigate a range of different compliance and buckling objective functions for maximizing the buckling resistance of a snap-through beam structure. It was demonstrated that due to the intrinsic nonlinear nature of the problem the load level, at which the compliance objective function is evaluated, has a tremendous effect on the resulting optimized design and thus its structural performance. The chosen load level for the compliance objective specifies a certain displacement configuration such that the structure stiffness is maximized for that particular displacement configuration. This means that special care should be taken when choosing a load level, and thus a displacement configuration, for the compliance optimization, as demonstrated by optimization 1-3 in the numerical studies. More importantly, if the displacement configuration for the objective evaluation changes during the optimization, e.g. the end load becomes larger than a limit point load, as studied by optimization 3, there is a likelihood that the final structure will be unstable and thus a stiffer and stable structure may exist, which has a completely different displacement

configuration, for the same load level. This problem is especially evident when changing the penalization parameter p in a continuation approach as observed in the numerical studies.

During topology optimization critical points, i.e. bifurcation and limit points, may be introduced and a pure end compliance objective at a fixed load may be insufficient if such points are not captured and dealt with. An overlooked bifurcation point may result in stiffness maximization of a non-physical displacement configuration while a limit point may result in stiffness maximization of a postbuckling displacement configuration. By including special features within the nonlinear path tracing analysis critical points may be detected and the end load level for the compliance objective evaluation may then be chosen accordingly. From the optimization studies, it was found that compliance minimization at a displacement configuration near the limit point load is a good criterion for maximizing the limit point load when the equilibrium path is carefully monitored for not having bifurcation points.

Symmetry is potentially dangerous to enforce in order to reduce model size when performing topology optimization of geometrically nonlinear structures. During the numerical studies it has been verified how an initial symmetric buckling response, in which symmetry considerations are perfectly valid, may change to an asymmetric buckling response during the optimization process. By enforcing symmetry, the asymmetric response is ignored, and thus a potentially false displacement configuration may be optimized. The use of symmetry in topology optimization of geometrically nonlinear structures should in general be avoided and if used the complete optimized design should be carefully analyzed and assessed.

A nonlinear buckling optimization formulation has been introduced for topology optimization of geometrically nonlinear structures experiencing a general type of instability, i.e. bifurcation or limit point instability. From the numerical studies the proposed formulation reliably improved the nonlinear buckling load and effectively handled “mode switching” and stability points that are introduced during the optimization process. To avoid artificial buckling modes in the nonlinear eigenvalue buckling problem, and retain consistency within the static geometrically nonlinear problem and design sensitivity analysis, a modified material interpolation scheme is proposed. This material interpolation scheme avoids problems with artificial buckling modes but results in slow convergence behaviour. The latter is believed to be caused by the fact that standard SIMP not uniquely penalizes intermediate densities in the buckling problem contrary to the compliance problem. The intended unfavourable relation between mass and stiffness for intermediate densities in the compliance problem does not necessarily apply to the buckling problem. This may immediately be realized

by considering the fact that the design sensitivities in the buckling problem can attain both negative and positive values. Thus, it may be advantageous to remove material which also means that higher penalization may in fact increase the buckling load. We believe that in order to obtain better convergence properties when using buckling as objective, specialized material interpolation schemes that implicitly penalize the buckling problem in regions of intermediate densities are needed. This is an important subject that demands further research.

Acknowledgements The authors gratefully acknowledge the support from the Danish Center for Scientific Computing (DCSC) for the hybrid Linux Cluster “Fyrkat” at Aalborg University, Denmark.

References

- Bendsøe MP (1989) Optimal shape design as a material distribution problem. *Struct Multidisc Optim* 1(4):193–202
- Bendsøe MP, Kikuchi N (1988) Generating optimal topologies in structural design using a homogenization method. *Comp Meth App Mech Eng* 71:197–224
- Bendsøe MP, Sigmund O (1999) Material interpolation schemes in topology optimization. *Arch Appl Mech* 69:635–654
- Bendsøe MP, Sigmund O (2003) *Topology optimization - theory, methods and applications*, 2nd edn. Springer Verlag Berlin Heidelberg New York, ISBN: 3-540-42992-1
- Bendsøe MP, Olhoff N, Taylor JE (1983) A variational formulation for multicriteria structural optimization. *J Struct Mech* 11:523–544
- Borri C, Hufendiek HW (1985) Geometrically nonlinear behaviour of space beam structures. *J Struct Mech* 13:1–26
- Brendel B, Ramm E (1980) Linear and nonlinear stability analysis of cylindrical shells. *Compt Struct* 12:549–558
- Bruns TE, Sigmund O (2004) Toward the topology design of mechanisms that exhibit snap-through behavior. *Comput Methods Appl Mech Engrg* 193:3973–4000
- Bruns TE, Sigmund O, Tortorelli DA (2002) Numerical methods for the topology optimization of structures that exhibit snap-through. *Int J Numer Meth Engrg* 55:1215–1237
- Buhl T, Pedersen CBW, Sigmund O (2000) Stiffness design of geometrically nonlinear structures using topology optimization. *Struct Multidisc Optim* 19:93–104
- Courant R, Hilbert D (1953) *Methods of mathematical physics, vol 1*. New York : Interscience Publishers
- Crisfield MA (1981) A fast incremental/iterative solution procedure that handles “snap-through”. *Compt Struct* 13:55–62
- Du J, Olhoff N (2007) Topological design of freely vibrating continuum structures for maximum values of simple and multiple eigenfrequencies and frequency gaps. *Struct Multidisc Optim* 34:91–110, DOI 10.1007/s00158-007-0101-y
- Hinton E (ed) (1992) *NAFEMS Introduction to Nonlinear Finite Element Analysis*. Bell and Bain Ltd, Glasgow, ISBN 1-874376-00-X
- Kemmler R, Lipka A, Ramm E (2005) Large deformations and stability in topology optimization. *Struct Multidisc Optim* 30:459–476
- Khot NS, Venkayya VB, Berke L (1976) Optimal structural design with stability constraints. *Int J Numer Methods Eng* 10:1097–1114
- Lee SJ, Hinton E (2000) Dangers inherited in shells optimized with linear assumptions. *Compt Struct* 78:473–486
- Lindgaard E, Lund E (2010) Nonlinear buckling optimization of composite structures. *Compt Methods Appl Mech Engrg* 199(37-40):2319–2330, DOI 10.1016/j.cma.2010.02.005

Lindgaard E, Lund E (2011) A unified approach to nonlinear buckling optimization of composite structures. *Compt Struct* 89(3-4):357–370, DOI 10.1016/j.compstruc.2010.11.008

Lindgaard E, Lund E, Rasmussen K (2010) Nonlinear buckling optimization of composite structures considering “worst” shape imperfections. *Int J Solids Struct* 47(22-23):3186–3202, DOI 10.1016/j.ijsolstr.2010.07.020

Lund E, Stegmann J (2005) On structural optimization of composite shell structures using a discrete constitutive parametrization. *Wind Energy* 8:109–124, DOI 10.1002/we.132

Manickarajaha D, Xiea YM, Steven GP (2000) Optimisation of columns and frames against buckling. *Compt Struct* 75:45–54

Min S, Kikuchi N (1997) Optimal reinforcement design of structures under the buckling load using the homogenization design method. *Struct Eng Mech* 5:565–576

Neves MM, Rodrigues H, Guedes JM (1995) Generalized topology design of structures with a buckling load criterion. *Struct Optim* 10:71–78

Neves MM, Sigmund O, Bendsoe MP (2002) Topology optimization of periodic microstructures with a penalization of highly localized buckling modes. *Int J Numer Meth Engng* 54:809–834

Olhoff N (1989) Multicriterion structural optimization via bound formulation and mathematical programming. *Struct Optim* 1:11–17

Olhoff N, Rasmussen SH (1977) On single and bimodal optimum buckling loads of clamped columns. *Int J Solids Struct* 13:605–614

Rozvany GIN, Zhou M, Birker T (1992) Generalized shape optimization without homogenization. *Struct Multidisc Optim* 4(3-4):250–252

Sekimoto T, Noguchi H (2001) Homologous topology optimization in large displacement and buckling problems. *JSME Int J* 44:616–622

Seyranian AP, Lund E, Olhoff N (1994) Multiple eigenvalues in structural optimization problems. *Struct Optim* 8:207–227

Svanberg K (1987) Method of moving asymptotes - a new method for structural optimization. *Int J Numer Methods Eng* 24:359–373

Taylor JE, Bendsoe MP (1984) An interpretation of min-max structural design problems including a method for relaxing constraints. *Int J Solids Struct* 20(4):301–314

Wilson EL, Itoh T (1983) An eigensolution strategy for large systems. *Compt Struct* 16:259–265

Wittrick WH (1962) Rates of change of eigenvalues, with reference to buckling and vibration problems. *J Roy Aeronaut Soc* 66:590–591

A Design sensitivity analysis

A.1 Sensitivity of linear displacements

The displacement sensitivities $\frac{d\mathbf{D}}{d\rho_e}$ are computed by direct differentiation of the static equilibrium equation, (1), w.r.t. a design variable ρ_e , $e = 1, \dots, N_e$.

$$\mathbf{K}_0 \frac{d\mathbf{D}}{d\rho_e} = -\frac{d\mathbf{K}_0}{d\rho_e} \mathbf{D} + \frac{d\mathbf{R}}{d\rho_e}, \quad e = 1, \dots, N_e \quad (20)$$

The displacement sensitivity $\frac{d\mathbf{D}}{d\rho_e}$ can be evaluated by backsubstitution of the factored global initial stiffness matrix in (20). The initial stiffness matrix has already been factored when solving the static problem in (1) and can here be reused, whereby only the new terms on the right hand side of (20), called the pseudo load vector, need to be calculated. Note that the force vector derivative, $\frac{d\mathbf{R}}{d\rho_e}$, is zero for design independent loads. The global initial stiffness matrix derivative $\frac{d\mathbf{K}_0}{d\rho_e}$ only involve the derivative of the current local element stiffness matrix $\frac{d\mathbf{K}_0}{d\rho_e}$ which is

determined by central difference approximations at the element level. The element stiffness derivative could easily be evaluated analytically, however for ease of programming a semi-analytical approach has been used.

A.2 Sensitivity of nonlinear displacements

The sensitivities of nonlinear displacements are computed by considering the residual or force unbalance equation at a converged load step n ,

$$\mathbf{Q}^n(\mathbf{D}^n(\boldsymbol{\rho}), \boldsymbol{\rho}) = \mathbf{F}^n - \mathbf{R}^n = \mathbf{0} \quad (21)$$

where $\mathbf{Q}^n(\mathbf{D}^n(\boldsymbol{\rho}), \boldsymbol{\rho})$ is the so-called residual or force unbalance, \mathbf{F}^n is the global internal force vector, and \mathbf{R}^n is the global applied load vector. Taking the total derivative of this equilibrium equation with respect to any of the design variables ρ_e , $e = 1, \dots, N_e$, we obtain

$$\frac{d\mathbf{Q}^n}{d\rho_e} = \frac{\partial \mathbf{Q}^n}{\partial \rho_e} + \frac{\partial \mathbf{Q}^n}{\partial \mathbf{D}^n} \frac{d\mathbf{D}^n}{d\rho_e} = \mathbf{0} \quad (22)$$

$$\text{where } \frac{\partial \mathbf{Q}^n}{\partial \mathbf{D}^n} = \frac{\partial \mathbf{F}^n}{\partial \mathbf{D}^n} - \frac{\partial \mathbf{R}^n}{\partial \mathbf{D}^n} \quad (23)$$

$$\text{and } \frac{\partial \mathbf{Q}^n}{\partial \rho_e} = \frac{\partial \mathbf{F}^n}{\partial \rho_e} - \frac{\partial \mathbf{R}^n}{\partial \rho_e} \quad (24)$$

We note that (23) reduces to the tangent stiffness matrix. Since it is assumed that the current load is independent of deformation, $\frac{\partial \mathbf{R}^n}{\partial \mathbf{D}^n} = \mathbf{0}$, we obtain

$$\frac{\partial \mathbf{F}^n}{\partial \mathbf{D}^n} = \mathbf{K}_T^n \quad (25)$$

By inserting the tangent stiffness and (24) into (22), we obtain the displacement sensitivities $\frac{d\mathbf{D}^n}{d\rho_e}$ as

$$\mathbf{K}_T^n \frac{d\mathbf{D}^n}{d\rho_e} = \frac{\partial \mathbf{R}^n}{\partial \rho_e} - \frac{\partial \mathbf{F}^n}{\partial \rho_e} \quad (26)$$

The partial derivative of the load vector, $\frac{\partial \mathbf{R}^n}{\partial \rho_e}$, can explicitly be expressed by two terms by taking the partial derivative of (6)

$$\frac{\partial \mathbf{R}^n}{\partial \rho_e} = \gamma^n \frac{\partial \mathbf{R}}{\partial \rho_e} + \frac{\partial \gamma^n}{\partial \rho_e} \mathbf{R} \quad (27)$$

For design independent loads $\frac{\partial \mathbf{R}}{\partial \rho_e} = \mathbf{0}$ and for a fixed load level $\frac{\partial \gamma^n}{\partial \rho_e} = 0$. The pseudo load vector, i.e. the right hand side of (26), is determined at the element level by central difference approximations and assembled to global vector derivatives. Again, the partial derivative only involves the element which is associated with the current design variable.

A.3 Linear compliance

The design sensitivity of linear compliance is obtained by the adjoint approach, see e.g. Bendsoe and Sigmund (2003); Lund and Stegmann (2005). The sensitivity with respect to any design variable ρ_e , $e = 1, \dots, N_e$ is

$$\frac{dC_L}{d\rho_e} = -\mathbf{D}^T \frac{d\mathbf{K}_0}{d\rho_e} \mathbf{D} \quad (28)$$

The global initial stiffness matrix derivatives $\frac{d\mathbf{K}_0}{d\rho_e}$ are determined semi-analytically at the element level by central difference approximations and assembled to global matrix derivatives.

A.4 Nonlinear end compliance

The design sensitivity of nonlinear end compliance at a converged load step n with respect to any design variable, $\rho_e, e = 1, \dots, N_e$, is obtained by the adjoint approach, see e.g. Bendsøe and Sigmund (2003)

$$\frac{dC_{GNL}}{d\rho_e} = \boldsymbol{\lambda}^T \frac{\partial \mathbf{Q}^n}{\partial \rho_e} = \boldsymbol{\lambda}^T \left(\frac{\partial \mathbf{F}^n}{\partial \rho_e} - \frac{\partial \mathbf{R}^n}{\partial \rho_e} \right) \quad (29)$$

Assuming the end load fixed and independent of design changes we have that $\frac{\partial \mathbf{R}^n}{\partial \rho_e} = \mathbf{0}$. The adjoint vector $\boldsymbol{\lambda}$, which is not to be confused with the eigenvector, is obtained as the solution to the adjoint equation

$$\mathbf{K}_T^n \boldsymbol{\lambda} = -\mathbf{R}^n \quad (30)$$

The partial derivatives in the right hand side of (29) are determined at the element level by central difference approximations and assembled to global vector derivatives.

A.5 Linear buckling

The linear buckling load factor sensitivities are determined by

$$\frac{d\lambda_j}{d\rho_e} = \boldsymbol{\phi}_j^T \left(\frac{d\mathbf{K}_0}{d\rho_e} + \lambda_j \frac{d\mathbf{K}_\sigma}{d\rho_e} \right) \boldsymbol{\phi}_j \quad (31)$$

where the eigenvalue problem in (2) has been differentiated with respect to any design variable, $\rho_e, e = 1, \dots, N_e$, assuming that λ_j is simple, see e.g. Courant and Hilbert (1953); Wittrick (1962). The global matrix derivatives of \mathbf{K}_0 and \mathbf{K}_σ are determined semi-analytically at the element level by central difference approximations and assembled to global matrix derivatives. The stress stiffness matrix is an implicit function of the displacement field, i.e. $\mathbf{K}_\sigma(\mathbf{D}(\boldsymbol{\rho}), \boldsymbol{\rho})$, and thus depends on all elements within the model. Both displacement field and design variables need to be perturbed in the element central difference approximation. The displacement field is perturbed via the calculated displacement sensitivities in (20) such that $\Delta \mathbf{D} \approx \frac{d\mathbf{D}}{d\rho_e} \Delta \rho_e$.

A.6 Nonlinear buckling

The nonlinear buckling load factor sensitivities at load step n are determined by

$$\frac{d\lambda_j}{d\rho_e} = \boldsymbol{\phi}_j^T \left(\frac{d\mathbf{K}_0}{d\rho_e} + \frac{d\mathbf{K}_L^n}{d\rho_e} + \lambda_j \frac{d\mathbf{K}_\sigma^n}{d\rho_e} \right) \boldsymbol{\phi}_j \quad (32)$$

and

$$\frac{d\gamma_j^c}{d\rho_e} = \frac{d\lambda_j}{d\rho_e} \gamma_j^n \quad (33)$$

where the eigenvalue problem in (11) has been differentiated with respect to any design variable, $\rho_e, e = 1, \dots, N_e$, assuming that λ_j is simple, see Lindgaard and Lund (2010). It is assumed that the final load level is fixed and that the nonlinear buckling load has been determined at load step n by evaluation of (10) and (11). The global matrix derivatives of \mathbf{K}_0 , \mathbf{K}_L^n , and \mathbf{K}_σ^n are determined in the same manner as for the linear buckling load sensitivities, i.e. semi-analytical central difference approximations at the element level and assembly to global matrix derivatives. The displacement field is perturbed via the calculated sensitivities of the nonlinear displacements in (26) such that $\Delta \mathbf{D}^n \approx \frac{d\mathbf{D}^n}{d\rho_e} \Delta \rho_e$.